

Seismic Travel Time Evidence for Lateral Inhomogeneity in the Deep Mantle

BRUCE R. JULIAN & MRINAL K. SENGUPTA

Lincoln Laboratory, Massachusetts Institute of Technology, Lexington, Massachusetts 02173

We present evidence from seismic travel time data of lateral variations in the properties of the lower mantle. The size of some anomalies is about 1,000 km.

EVIDENCE from seismic body wave and surface wave data has long indicated that the Earth's upper mantle (depth < 700 km) is strongly laterally heterogeneous. Lateral variations of the compressional wave velocity as large as 10% have been reported for the upper 200 km, and the shear velocity probably varies even more. For depths greater than 700 km, however, the existence of lateral variations has been more difficult to establish, although such variations have been invoked by various workers^{1,2} to explain the scatter of some seismological data. Greenfield and Sheppard³, in a study of $dT/d\Delta$ measurements made at the Large Aperture Seismic Array in Montana, found a pronounced difference between data from events to the northwest and the southeast for epicentral distances greater than 60°, which could not be attributed to the structure beneath the array, and seems explicable only in terms of heterogeneities in the lower mantle. Davies and Sheppard⁴ have presented a more extensive collection of data of this type in the form of an "array diagram", on which $dT/d\Delta$ and azimuth anomalies are represented as vectors in slowness space. Many anomalies are found which are too large to be effects of upper mantle heterogeneities in the source regions; on the other hand, the anomalies often vary rapidly with the direction of approach of the waves, implying that structure directly beneath the array is not responsible. Further evidence has come from a study of the diffraction of compressional waves by the Earth's core, in which Alexander and Phinney⁵ found that the region of the core-mantle boundary beneath the Pacific Basin is distinctly different from the region beneath the North Atlantic and Africa.

Travel Time Anomalies

We have found evidence that significant lateral variations occur in the lowest few hundred km of the mantle, this region being much more heterogeneous than that which lies above it. The methods of this travel time study are described in detail elsewhere⁶.

We restricted the study to data from deep focus earthquakes in an attempt to avoid systematic errors caused by near source velocity variations in the upper mantle, which are particularly severe in seismically active regions. About 3,300 arrival time data from 47 earthquakes with depths between 450 and 650 km were used, all events being located in the deepest parts of their

respective seismic zones. For most of the 18 seismic regions involved, two or more events were available, and for each station a consistency check was made to eliminate data contaminated by gross errors. An iterative procedure, similar to the one described by Herrin *et al.*⁷, was then used to determine the earthquake locations, the travel time curve for a 550 km focal depth, and a set of "station corrections" (each represented by a constant) to account for the effect of lateral variations in the upper mantle beneath the stations.

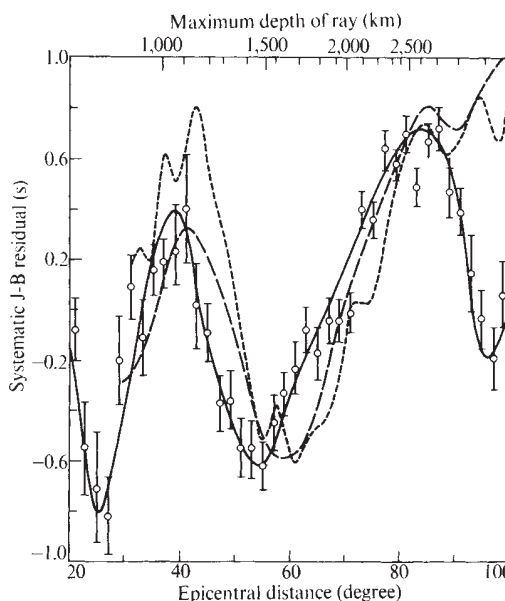


Fig. 1 P wave travel time curve (focal depth 550 km) determined in this study (—), expressed in terms of deviations from the Jeffreys-Bullen values. Data means and their standard errors are indicated for 2° distance intervals. Surface focus curves of Herrin *et al.*⁷ (---) and Lilwal and Douglas⁸ (- - -) have been displaced vertically for ease of comparison.

The travel time curve thus determined is shown in Fig. 1 (in terms of deviation from the standard Jeffreys-Bullen tables), together with the data means and their standard errors for 2° distance intervals. This curve is similar in shape to those found in other recent studies^{7,8} except beyond 85°, where most other curves remain approximately parallel to the Jeffreys-Bullen curve, but ours becomes progressively earlier by about 0.9 s. Fig. 2 shows some of the data which have contributed to the determination of the travel time curve; the observed times show a striking dependence upon the location of the earth-

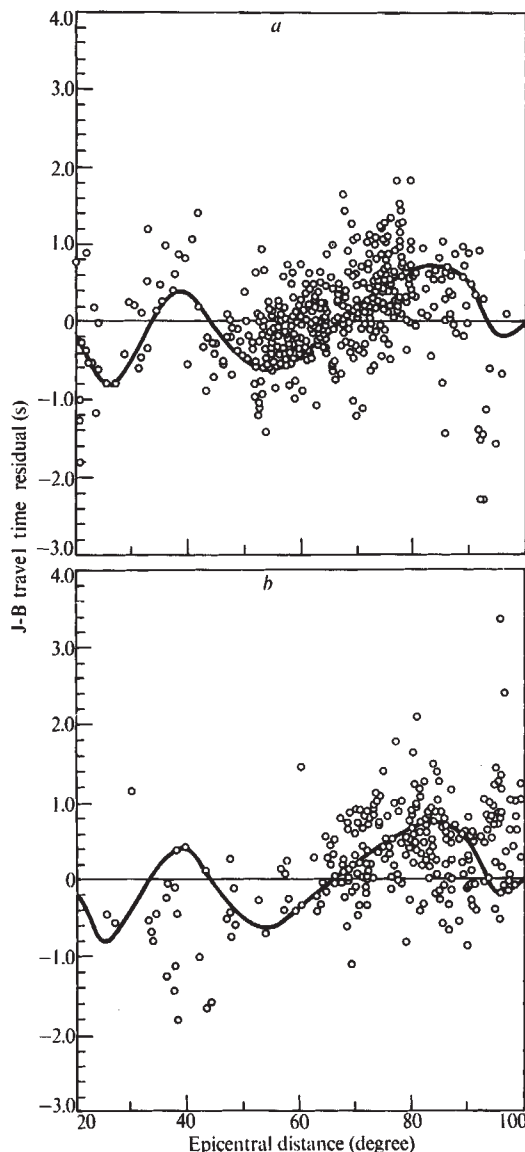


Fig. 2 Travel time data (with station corrections applied) for earthquakes in (a) the Sea of Okhotsk and (b) Argentina. The solid line is the curve derived from all data.

quakes. The difference between the curves in Fig. 1 results from differences in the geographic regions sampled. Possible causes of a regional dependence of this nature are velocity variations in the upper mantle in the source or receiver regions or in the lower mantle, and mislocation of the events (caused by uneven station distribution, and so on). Event mislocation and structure in the receiver regions can be ruled out because they would be expected to produce similar effects at all epicentral distances. Although the observed variations are most striking beyond 85° , we shall show that they are much smaller at distances less than 70° . It is conceivable that structure in the source regions could produce a distance dependent regional variation of this kind, if the velocity anomalies were systematically located relative to the earthquake hypocentres (as indeed they are beneath island arcs). In that case the variations would have to be localized in a very small region beneath the hypocentres, because a 10° distance interval maps into about a 5° difference in angle at the focus. Even if the anomalous regions are as deep as 1,000 km, the velocity change must occur over a horizontal distance of only 50 km or so. This possibility may be ruled out because all the earthquakes in each source region yield a similar pattern of travel time residuals, even though the epicentre locations in each region are typically distributed over > 200 km. Velocity

variations near the focus are further ruled out because early arrivals beyond 85° are not restricted to observations of deep earthquakes; they also occur, for example, in data from nuclear explosions in the Marshall Islands⁹.

Deep Mantle Structure

It seems, then, that lateral variations of compressional velocity in the middle or lower mantle are required to explain the travel time anomalies. But because of the uneven distribution of seismological observatories and deep earthquakes, the sampling of the mantle provided by available data is uneven, and it is impossible to determine uniquely the complete three dimensional velocity structure of the mantle. What can be determined is the average travel time residual for each of a number of "bundles" of rays following nearly identical paths from a seismic region to a group of stations, and from this information we infer the most probable cause of the variations. Table 1 summarizes the travel time data for all paths for which 9 or more observations are available. For each path a Student's t test has been used to evaluate the hypothesis that the mean travel time (after station corrections have been applied) is the value given by the curve in Fig. 1 and that deviations from this curve can be attributed to random measuring errors. Those ray paths for which the hypothesis could be rejected at the 99.5% confidence level are indicated in Table 1. Fig. 3 shows histograms of the residual distribution for these anomalous paths. For observations at distances beyond 70° , 16 paths (out of 34 tested) showed significant variations from the average curve, whereas for smaller distances, only 3 anomalous paths (out of 22) were found. This strongly suggests that most of the scatter originates in the deep mantle (depth $> 2,000$ km). The possibility of the variations occurring at a shallower depth

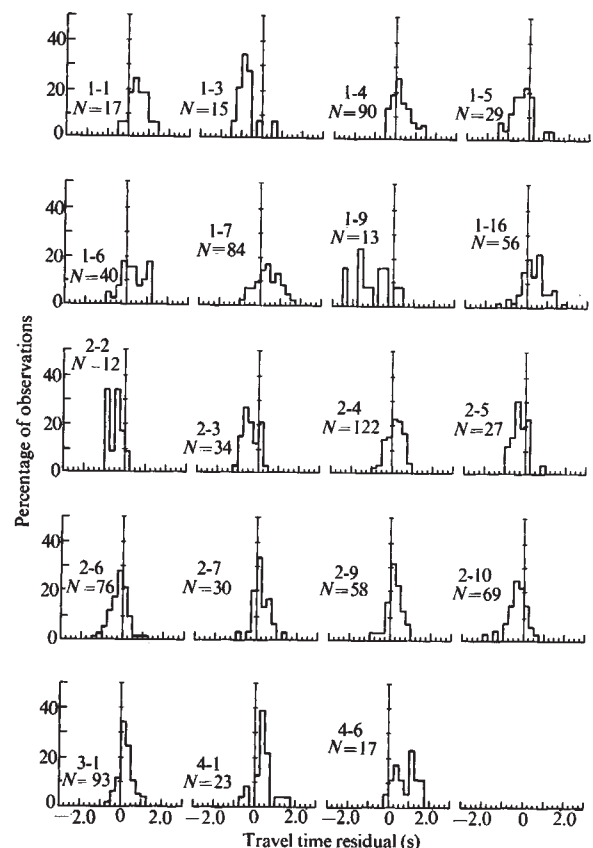


Fig. 3 Histograms of travel time residuals (relative to curve of Fig. 1 with station corrections applied) for different ray paths through the mantle. Identification numbers correspond to those in Table 1 and Fig. 4. N is the number of observations.

Table 1 Travel Time Statistics for Mantle P Wave Paths

Identifica- tion No.	<i>N</i>	\bar{x}	<i>s</i>	<i>t</i>	<i>t</i> _{99.5}	Path
(a) 85° < Δ < 100°						
1-1*	17	0.46	0.43	4.41	3.25	Japan—USA
1-2	12	-0.11	0.56	-2.15	3.50	Bonin and Marianas Arc—USA
1-3*	15	-0.76	0.48	-6.13	3.33	Tonga Arc—Alaska
1-4*	90	0.23	0.50	4.37	2.89	Tonga Arc—Western North America
1-5*	29	-0.34	0.57	-3.21	3.05	Argentina—Western North America
1-6*	40	0.37	0.70	3.34	2.97	South America—Northwestern Europe
1-7*	84	0.38	0.79	4.40	2.89	South America—Southern Europe
1-8	11	0.06	0.56	0.36	3.58	South America—Southern Africa
1-9*	13	-1.09	0.91	-4.31	3.43	Kuril Arc—Spain, Morocco and Algeria
1-10	16	-0.36	0.58	-2.48	3.29	Bonin Arc—Europe
1-11	42	-0.19	0.65	-1.90	2.97	Indonesia and Philippine Is.—Central and Northern Europe
1-12	14	0.16	0.48	1.25	3.37	Indonesia and Philippine Is.—Middle East and Balkans
1-13	13	0.47	0.96	1.77	3.43	Indonesia and Philippine Is.—Central and Southern Africa
1-14	10	-0.12	0.56	-0.68	3.69	Tonga Arc—Siberia and China
1-15	9	-0.24	0.28	-2.57	3.83	Indonesia—Alaska
1-16*	56	0.34	0.61	4.17	2.92	Solomon Is.—Western USA
1-17	29	0.04	0.33	0.65	3.05	New Hebrides—Western North America
(b) 70° < Δ < 85°						
2-1	57	-0.12	0.45	-2.02	2.92	Japan—USA
2-2*	12	-0.51	0.36	-4.90	3.45	Japan—Southwestern USA
2-3*	34	-0.38	0.37	-5.99	3.01	Bonin Arc—Western USA
2-4*	122	0.16	0.40	4.38	2.86	Tonga Arc—Western North America
2-5*	27	-0.27	0.39	-3.60	3.07	Kuril Arc—Eastern North America
2-6*	76	-0.19	0.45	-3.68	2.90	Argentina and Bolivia—Central and Western USA
2-7*	30	0.25	0.44	3.11	3.04	South America—Spain and Northern Africa
2-8	20	-0.09	0.45	-0.89	3.17	South America—Central and Southern Africa
2-9*	58	0.19	0.43	3.36	2.92	Kuril Arc—Western Europe
2-10*	69	-0.33	0.52	-5.28	2.91	Japan—Western Europe
2-11	22	0.02	0.36	0.26	3.14	New Hebrides—Western North America
2-12	20	-0.06	0.47	-0.57	3.17	Indonesia and Philippine Is.—Middle East
2-13	30	-0.09	0.52	-0.95	3.04	Bonin and Marianas Arcs—Scandinavia and Western Russia
2-14	23	0.14	0.38	1.77	3.12	Japan and Kuril Arc—Australia
2-15	11	-0.06	0.54	-0.37	3.58	Kuril Arc—Middle East
2-16	12	-0.39	0.56	-2.41	3.50	Indonesia—Antarctica
2-17	10	-0.22	0.25	-2.78	3.69	Marianas Arc—Western USA
2-18	12	-0.22	0.69	-1.10	3.50	Japan—Middle East
(c) 55° < Δ < 70°						
3-1*	93	0.23	0.38	5.84	2.89	Kuril Arc—Western USA
3-2	45	0.12	0.40	2.01	2.96	Northern South America—Western USA
3-3	42	0.06	0.49	0.79	2.97	Bolivia and Argentina—Central USA
3-4	93	-0.05	0.54	-0.89	2.89	Kuril Arc and Sea of Japan—Northern and Eastern Europe and Middle East
3-5	30	-0.09	0.41	-1.20	3.03	Indonesia and Philippine Is.—Southwestern Asia
3-6	15	0.18	0.62	1.12	3.33	Japan and Kuril Arc—Melanesia
3-7	12	-0.04	0.41	-0.34	3.43	Tonga Arc—Western Australia
3-8	10	-0.28	0.45	-1.97	3.58	Japan and Kuril Arc—Australia
3-9	9	-0.19	0.55	-1.04	3.69	New Hebrides—China and Siberia
3-10	8	0.13	0.78	0.47	4.03	Solomon Is.—Japan
3-11	15	0.26	0.47	2.14	3.29	Tonga Arc—Antarctica
3-12	9	0.22	0.58	1.14	3.69	Indonesia—New Zealand
3-13	10	0.15	0.59	0.80	3.58	Indonesia—Antarctica
(d) 40° < Δ < 55°						
4-1*	23	0.41	0.48	4.10	3.12	Kuril Arc—Northwestern North America
4-2	44	-0.18	0.48	-2.49	2.97	Northern South America—USA
4-3	15	0.35	0.41	3.31	3.33	Kuril Arc—Northern Europe
4-4	34	0.16	0.43	2.17	3.01	Japan—Southwestern Asia
4-5	17	-0.25	0.51	-2.02	3.22	Indonesia—India and Pakistan
4-6*	17	0.82	0.56	6.03	3.25	Japan—Alaska
4-7	13	-0.51	0.65	-2.82	3.37	Indonesia—Japan and Korea
4-8	40	0.02	0.55	0.23	2.97	Indonesia—Southeastern Australia and Tasmania
4-9	20	-0.06	0.58	-0.46	3.15	Solomon Is.—Japan, Korea, and Eastern China

N = Number of observations.

\bar{x} = Mean travel time residual after station correction (*s*).

s = Standard deviation of residuals (*s*).

$$t = \frac{\bar{x}}{s/\sqrt{N}}$$

*t*_{99.5} = 99.5% confidence limit for |*t*| if true mean is zero.

* Indicates paths with mean significantly different from zero.

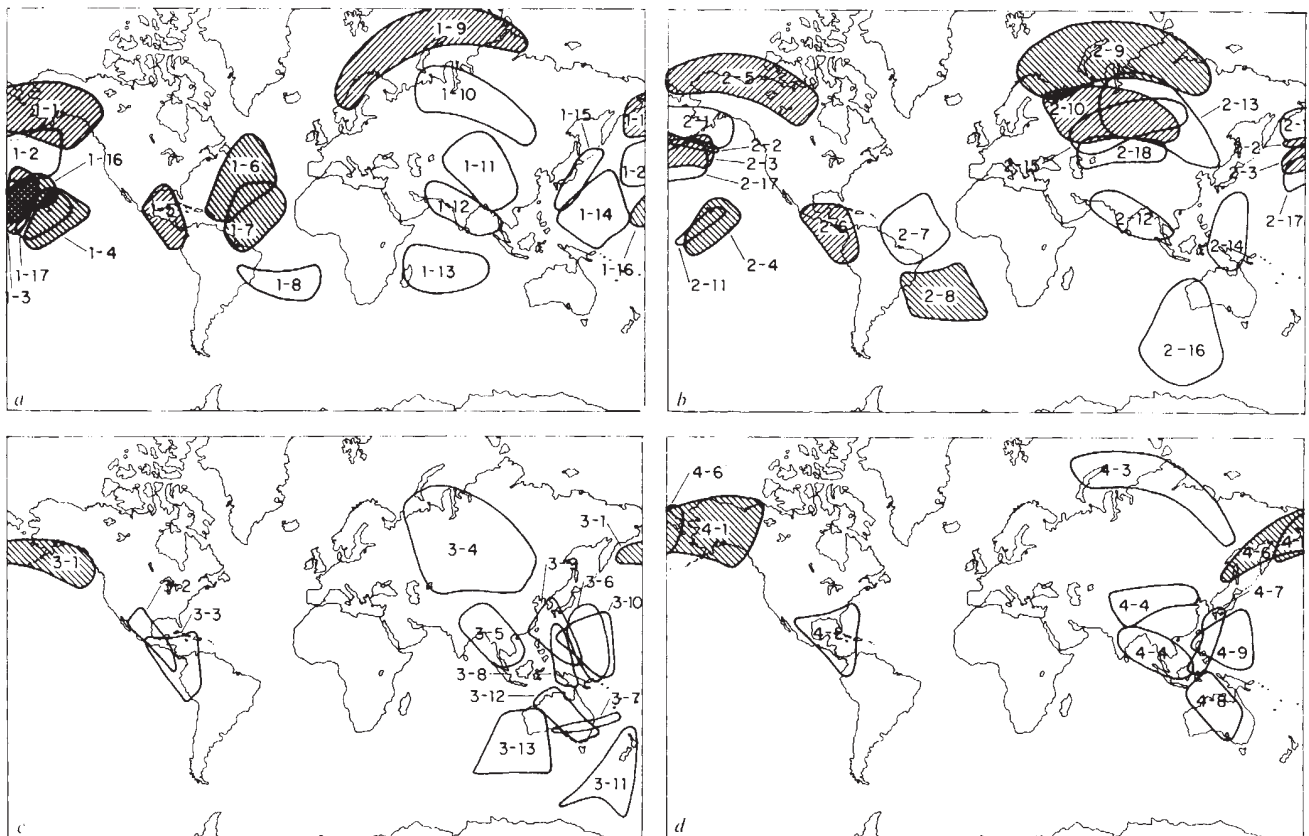


Fig. 4 Regions where paths of observed P waves bottom in the mantle. Cross-hatching indicates regions differing significantly from the mean determined from all data. Other regions tested are outlined. The identification numbers correspond to those in Table 1 and Fig. 3. ▨, Late; ▩, early.

cannot be absolutely disproved, but the velocity distribution in the Earth would have to be such that, given the distribution of earthquakes and seismic stations, all observed waves bottoming at the depth of the heterogeneities happen to be unaffected by them (even though P waves spend about 25% of their travel time traversing the lowest 10% of the ray path), while waves penetrating beneath the heterogeneities are affected. It seems unreasonable to assume such a conspiratorial behaviour on the part of the velocity variations when a much simpler hypothesis is available.

The actual details of the velocity distribution cannot, however, be determined precisely, because rays travel a great distance at approximately the same depth near their turning points. Fig. 4 shows the regions of the lower mantle sampled by the various ray bundles (defined arbitrarily as the central 30° of each path) and indicates which paths correspond to early and late arrivals. These are in most cases probably the regions where the actual velocity anomalies occur. Where regions overlap on the figure, they are generally consistent with each other (for example, regions 1-6 and 1-7, regions 2-2 and 2-3, and regions 4-1 and 4-6). This consistency is encouraging, in that it supports our argument that the travel time anomalies originate in the deep mantle and are not the result of some other type of systematic error. An apparent inconsistency exists between regions 1-3 and 1-16, but this is not surprising because of the uncertainty as to exactly where the travel time anomalies actually originate. The rays following path 1-3 also pass through regions 2-2 and 2-3 further to the north, and it is likely that the travel time anomaly actually originates there. Another interesting feature of Fig. 4 is a correlation between the anomalies in the two greatest distance ranges (for example, regions 1-7 and 2-7, regions 1-4 and 2-4, and regions 1-5 and 2-6), suggesting that the structure in the deep mantle has a spatial "coherence" of at least a few hundred km vertically.

The mean travel times in Table 1 show a variation of about 1.5 s for rays bottoming below 2,600 km, and about 0.6 s for rays bottoming between 2,000 and 2,600 km. These numbers are somewhat uncertain, but it is likely that the true travel times vary by at least 1 s. The amount by which the actual velocity in the mantle varies depends on the size of the regions within which the variations occur. The data of Fig. 4 suggest that the size of some of the anomalies, at least, is about 1,000 km or less, in which case the velocity must vary by at least 1%. This is a lower bound both because we have probably overestimated the scale of the inhomogeneities and because we are measuring averages of the velocity in rather large regions and some cancellation of the effects of positive and negative velocity anomalies is likely. Combined interpretation of travel time and $dT/d\Delta$ measurements can probably improve the resolution of structural details.

Might the deep mantle variations be related in some way to the convection plumes hypothesized by Wilson¹⁰ and Morgan¹¹ to exist in the deep mantle? To answer this the region of the Hawaiian Islands provides the best data, and here they indeed indicate a pronounced lateral variation, the velocities being high to the northwest of Hawaii (regions 2-2, 2-3, and probably 1-3) and low in the vicinity of the islands (regions 1-4, 2-4, and 1-6). Interestingly, the $dT/d\Delta$ data presented by Davies and Sheppard⁴ also indicate a horizontal velocity contrast of this sort in the vicinity of Hawaii. Unfortunately, no other proposed plumes are well sampled by our data. Region 1-13 includes the Mascarene Islands, but the data here are highly scattered, and no conclusion can be drawn. Regions 1-5 and 2-6, both with apparently high velocities, are located slightly to the northeast of the Galapagos Islands, so it is not clear what relation, if any, this velocity anomaly may bear to a possible plume. If travel time data for rays passing through more proposed plume regions can be obtained, they may

provide valuable evidence relevant to the Wilson–Morgan hypothesis.

Except, perhaps, for the Hawaiian Islands, no geological or tectonic features show an obvious correlation with the inferred deep mantle velocity anomalies. At shallower depths, however, this is not the case; regions 3–1, 4–1, and 4–6, all seeming to have low velocities, lie beneath the Kurile and Aleutian Island arcs. The only other island arc adequately sampled at these depths lies beneath Middle America (region 4–2) and is associated with early arrivals (though they are not significant at the 99.5% confidence level). The data thus suggest that low velocities may be characteristic of island arcs at depths greater than 1,000 km.

The data considered here do not support any correlation between velocity variations below 2,000 km and global gravity anomalies or geoid heights. At shallower depths such a correlation does exist, but it is merely another manifestation of the low velocities beneath the Kurile and Aleutian Islands, because the concave sides of island arcs are generally the sites of prominent positive free air gravity anomalies.

It is not possible to make a direct comparison between these results and those of Alexander and Phinney⁵. The region of the North Atlantic found by them to be anomalous is further east than the corresponding region sampled by our data. Further, travel time measurements such as ours provide a measure of

the average velocity in a region, whereas the behaviour of core diffracted waves depends on features such as the velocity gradient in the lower mantle. Further studies of variations in the “visibility” within the core shadow would be a useful complement to travel time and $dT/d\Delta$ studies of the lower mantle.

We thank Dr David Davies and Dr M. Nafi Toksöz for helpful suggestions. This work was sponsored by the Advanced Research Projects Agency of the Department of Defense.

Received January 2, 1973.

- ¹ Toksöz, M. Nafi, Chinnery, M. A., and Anderson, D. L., *Geophys. J. Roy. Astron. Soc.*, **13**, 31 (1967).
- ² Hales, A. L., and Roberts, J. L., *Bull. Seismol. Soc. Amer.*, **60**, 1427 (1970).
- ³ Greenfield, R. J., and Sheppard, R. M., *Bull. Seismol. Soc. Amer.*, **59** (1969).
- ⁴ Davies, D., and Sheppard, R. M., *Nature*, **239**, 318 (1972).
- ⁵ Alexander, Shelton S., and Phinney, R. A., *J. Geophys. Res.*, **7**, 5943 (1966).
- ⁶ Sengupta, Mrinal K., thesis, MIT (1972).
- ⁷ Herrin, E., Tucker, W., Taggart, J., Gordon, D. W., and Lobdell, J. L., *Bull. Seismol. Soc. Amer.*, **58**, 1273 (1968).
- ⁸ Lilwal, R. C., and Douglas, A., *Geophys. J. Roy. Astron. Soc.*, **19**, 165 (1970).
- ⁹ Carder, D. S., Gordon, D. W., and Jordan, J. N., *Bull. Seismol. Soc. Amer.*, **56**, 815 (1966).
- ¹⁰ Wilson, J. T., *Phil. Trans. Roy. Soc., A*, **258**, 145 (1965).
- ¹¹ Morgan, W. J., *Nature*, **230**, 42 (1971).

Evidence for an Advanced Plio-Pleistocene Hominid from East Rudolf, Kenya

R. E. F. LEAKEY

National Museums of Kenya, PO Box 40658, Nairobi

Four specimens collected last year from East Rudolf are provisionally attributed to the genus *Homo*. One, a cranium KNM-ER 1470, is probably 2.9 million years old.

PRELIMINARY descriptions are presented of four specimens collected from East Rudolf during 1972. Most of the collection recovered during this field season has been reported recently in *Nature*¹; the specimens described here are sufficiently important to be considered separately and in more detail. The collections of fossil hominids recovered from East Rudolf during earlier field seasons and detailed descriptions of some of these specimens have been published previously^{2–5}.

The specimens described here are: (1) a cranium, KNM-ER 1470; (2) a right femur, KNM-ER 1472; (3) a proximal fragment of a second right femur, KNM-ER 1475; and (4) an associated left femur, distal and proximal fragments of a left tibia, and a distal left fibula, KNM-ER 1481. They were all recovered from area 131 (see Fig. 1) and from deposits below the KBS Tuff which has been securely dated at 2.6 m.y.⁶.

Area 131 consists of approximately 30 km² of fluvial and lacustrine sediments. The sediments are well exposed and show no evidence of significant tectonic disturbance; there is a slight

westward dip of less than 3°. Several prominent marker horizons provide reference levels and have permitted physical correlation of stratigraphical units between area 131 and other areas in the East Rudolf locality.

Several tuffs occur in the vicinity of area 131. The lowest of these is the Tulu-Bor Tuff which is not exposed in the area itself but does outcrop nearby in several stream beds. Above this horizon, in a composite section, there is some 60 m of sediment capped by the prominent KBS Tuff. This latter tuff has been mapped into areas 108 and 105 (also shown in Fig. 1) from where samples have been obtained for K/Ar dates. An account of the geology is given by Vondra and Bowen⁷. A section showing the vertical position of these four hominids in relation to the KBS Tuff is given in Fig. 2.

At present, analysis of samples collected for dating from the KBS Tuff in area 131 has proved inconclusive because of the apparent alteration of the sanidine feldspars. This was not seen in the 105/108 samples from the same horizon which provided the date of 2.61 m.y. and there is no reason to suspect the validity of that date (personal communication from J. A. Miller).

Detailed palaeomagnetic investigation of the sedimentary units is being undertaken by Dr A. Brock (University of Nairobi). Systematic sampling closely spaced in the section has identified both the Mammoth and Kaena events in area 105 between the Tulu-Bor and KBS Tuffs, a result which supports the 2.61 m.y. date on the latter. The mapping of several